

# Dark $SU(2) \rightarrow Z_3 \times Z_2$ Gauge Symmetry

**Debasish Borah**

*Department of Physics, Indian Institute of Technology Guwahati, Assam 781039, India*

**Ernest Ma**

*Department of Physics and Astronomy,  
University of California, Riverside, California 92521, USA*

**Dibyendu Nanda**

*School of Physics, Korea Institute for Advanced Study, Seoul 02455, Korea*

## Abstract

The dark sector is postulated to be invariant under an  $SU(2)$  gauge symmetry, spontaneously broken by a Higgs quadruplet to a conserved residual  $Z_3 \times Z_2$  symmetry. The resulting dark matter phenomenology is studied.

## I. INTRODUCTION

Whereas the stability of dark matter (DM) [1] is most likely due to an unbroken symmetry [2, 3], its nature and its origin are both unknown. It may well have something to do with a non-Abelian gauge symmetry, the simplest of which is  $SU(2)$  [4]. The associated gauge bosons are presumably heavy from the spontaneous breaking of the gauge symmetry through Higgs scalars. If a Higgs doublet is used, then the resulting theory has a residual  $SU(2)$  global symmetry [4, 5]. If both a doublet and a triplet are used, then the breaking may be gauge  $SU(2)$  to gauge  $U(1)$  to global  $U(1)$  [6]. If other scalar multiplets are used, there are various possible outcomes [7]. In this paper, we study in detail the case of a Higgs  $SU(2)$  quadruplet [8], resulting in a dark discrete  $Z_3$  symmetry [9–11]. We show that an extra  $Z_2$  symmetry emerges as the result of the structure of this particular scalar potential, which was not recognized previously. We identify the possible dark matter candidates and study their phenomenology in relic abundance and direct detection. We note that the idea of gauge  $SU(2)$  family symmetry breaking to  $A_4$  using a Higgs septuplet has also been studied [12].

## II. THE MODEL

Consider the origin of dark matter as coming from an  $SU(2)$  gauge symmetry, broken by a Higgs quadruplet  $\Phi$ . The complete scalar potential involving  $\Phi$  is given by

$$\begin{aligned}
 V = & -\mu^2 \Phi^\dagger \Phi + \frac{1}{2} \lambda_1 (\Phi^\dagger \Phi)^2 - \frac{10}{9} \lambda_2 (\Phi \tilde{\Phi})_3 (\Phi \tilde{\Phi})_3 \\
 & - \left[ \frac{5}{18} \lambda_3 (\Phi \Phi)_3 (\Phi \Phi)_3 + \frac{5}{9} \lambda_4 (\Phi \Phi)_3 (\Phi \tilde{\Phi})_3 + \text{h.c.} \right].
 \end{aligned} \tag{1}$$

To justify the above, let  $\Phi = (\phi_3, \phi_2, \phi_1, \phi_0)$ , then the only quadratic invariant is  $\Phi^\dagger \Phi$ . Now  $(\Phi\Phi)_1 = (\Phi\Phi)_5 = 0$ , whereas

$$(\Phi\Phi)_3 = \begin{pmatrix} \sqrt{\frac{3}{10}}\phi_3\phi_1 - \sqrt{\frac{2}{5}}\phi_2\phi_2 + \sqrt{\frac{3}{10}}\phi_1\phi_3 \\ \sqrt{\frac{9}{20}}\phi_3\phi_0 - \sqrt{\frac{1}{20}}\phi_2\phi_1 - \sqrt{\frac{1}{20}}\phi_1\phi_2 + \sqrt{\frac{9}{20}}\phi_0\phi_3 \\ \sqrt{\frac{3}{10}}\phi_2\phi_0 - \sqrt{\frac{2}{5}}\phi_1\phi_1 + \sqrt{\frac{3}{10}}\phi_0\phi_2 \end{pmatrix}, \quad (2)$$

and

$$(\Phi\Phi)_3(\Phi\Phi)_3 = \frac{3}{5}(6\phi_0\phi_1\phi_2\phi_3 - 3\phi_0^2\phi_3^2 + \phi_1^2\phi_2^2) - \frac{4\sqrt{3}}{5}(\phi_0\phi_2^3 + \phi_1^3\phi_3). \quad (3)$$

As for  $(\Phi\Phi)_7$ , it may be neglected because  $(\Phi\Phi)_7(\Phi\Phi)_7 = -(\Phi\Phi)_3(\Phi\Phi)_3$ .

Consider now  $\tilde{\Phi} = (\phi_0^*, -\phi_1^*, \phi_2^*, -\phi_3^*)$ , which transforms as  $\Phi$ .

$$(\Phi\tilde{\Phi})_3 = \begin{pmatrix} \sqrt{\frac{3}{10}}\phi_3\phi_2^* + \sqrt{\frac{2}{5}}\phi_2\phi_1^* + \sqrt{\frac{3}{10}}\phi_1\phi_0^* \\ -\sqrt{\frac{9}{20}}\phi_3\phi_3^* - \sqrt{\frac{1}{20}}\phi_2\phi_2^* + \sqrt{\frac{1}{20}}\phi_1\phi_1^* + \sqrt{\frac{9}{20}}\phi_0\phi_0^* \\ -\sqrt{\frac{3}{10}}\phi_2\phi_3^* - \sqrt{\frac{2}{5}}\phi_1\phi_2^* - \sqrt{\frac{3}{10}}\phi_0\phi_1^* \end{pmatrix}. \quad (4)$$

Hence

$$(\Phi\tilde{\Phi})_3(\Phi\tilde{\Phi})_3 = -\frac{1}{20}(3|\phi_0|^2 + |\phi_1|^2 - |\phi_2|^2 - 3|\phi_3|^2)^2 - \frac{1}{5}|\sqrt{3}\phi_0\phi_1^* + 2\phi_1\phi_2^* + \sqrt{3}\phi_2\phi_3^*|^2, \quad (5)$$

which is the same as  $-(\Phi^\dagger\Phi)_3(\Phi^\dagger\Phi)_3$ .

Finally,

$$\begin{aligned} (\Phi\Phi)_3(\Phi\tilde{\Phi})_3 &= \frac{9}{10}(\phi_1\phi_2 - \phi_0\phi_3)(|\phi_0|^2 - |\phi_3|^2) + \frac{3}{10}(\phi_1\phi_2 + 3\phi_0\phi_3)(|\phi_2|^2 - |\phi_1|^2) \\ &+ \frac{\sqrt{3}}{5}(\phi_2\phi_2\phi_2\phi_3^* - \phi_0^*\phi_1\phi_1\phi_1 + 3\phi_0\phi_1^*\phi_2\phi_2 - 3\phi_1\phi_1\phi_2^*\phi_3), \end{aligned} \quad (6)$$

which is the same as  $-(\Phi\Phi)_7(\Phi\tilde{\Phi})_7$ .

As  $\phi_0$  and  $\phi_3$  develop vacuum expectation values, a residual  $Z_3$  symmetry remains, maintained by  $\phi_1 \sim \omega$ ,  $\phi_2 \sim \omega^2$ , with  $\phi_{0,3} \sim 1$ , where  $\omega^3 = 1$ .

Let  $\langle\phi_{0,3}\rangle = v_{0,3}$ , then  $V$  is minimized with

$$0 = v_0[-\mu^2 + \lambda_1(v_0^2 + v_3^2) + \lambda_2(v_0^2 - v_3^2) + \lambda_3v_3^2 + (3/2)\lambda_4v_0v_3] - \lambda_4v_3^3/2, \quad (7)$$

$$0 = v_3[-\mu^2 + \lambda_1(v_0^2 + v_3^2) + \lambda_2(v_3^2 - v_0^2) + \lambda_3v_0^2 - (3/2)\lambda_4v_0v_3] + \lambda_4v_0^3/2. \quad (8)$$

Let  $v_D = \sqrt{v_0^2 + v_3^2}$ ,  $c = \cos \theta = v_0/v_D$ ,  $s = \sin \theta = v_3/v_D$ , then

$$\frac{\lambda_4}{2\lambda_2 - \lambda_3} = \frac{2sc(c^2 - s^2)}{c^4 + s^4 - 6s^2c^2} = \frac{1}{2} \tan 4\theta, \quad (9)$$

$$v_D^2 = \frac{2\mu^2}{2\lambda_1 + \lambda_3 + (\tan 4\theta/2 \tan 2\theta)(2\lambda_2 - \lambda_3)}. \quad (10)$$

The scalar masses and interactions are then functions of  $v_D$ ,  $\theta$ , and  $\lambda_{1,2,3}$ .

### A. Dark Sector Mass Spectrum and Interactions

The dark gauge bosons  $X_{1,2,3}$  interact with  $\Phi$  according to

$$\left| \partial \begin{pmatrix} \phi_3 \\ \phi_2 \\ \phi_1 \\ \phi_0 \end{pmatrix} - ig_D \begin{pmatrix} \frac{3}{2}X_3 & \frac{\sqrt{3}}{2}(X_1 - iX_2) & 0 & 0 \\ \frac{\sqrt{3}}{2}(X_1 + iX_2) & \frac{1}{2}X_3 & X_1 - iX_2 & 0 \\ 0 & X_1 + iX_2 & -\frac{1}{2}X_3 & \frac{\sqrt{3}}{2}(X_1 - iX_2) \\ 0 & 0 & \frac{\sqrt{3}}{2}(X_1 + iX_2) & -\frac{3}{2}X_3 \end{pmatrix} \begin{pmatrix} \phi_3 \\ \phi_2 \\ \phi_1 \\ \phi_0 \end{pmatrix} \right|^2. \quad (11)$$

The masses of  $X_{1,2,3}$  are

$$M_{1,2}^2 = \frac{3}{2}g_D^2v_D^2, \quad M_3^2 = \frac{9}{2}g_D^2v_D^2, \quad (12)$$

with  $c\phi_1 - s\phi_2^*$  and  $\sqrt{2}\text{Im}(c\phi_0 - s\phi_3)$  as the longitudinal components of  $(X_1 - iX_2)/\sqrt{2} \sim \omega$  and  $X_3 \sim 1$  respectively under  $Z_3$ . The orthogonal components  $\eta = s\phi_1 + c\phi_2^*$  and  $\phi_I = \sqrt{2}\text{Im}(s\phi_0 + c\phi_3)$  have masses

$$M_\eta^2 = \frac{2}{3}\lambda_2v_D^2 + \frac{1}{2}M_{\phi_I}^2, \quad M_{\phi_I}^2 = - \left[ 2\lambda_3 + \frac{\tan 4\theta}{\tan 2\theta}(2\lambda_2 - \lambda_3) \right] v_D^2. \quad (13)$$

The  $2 \times 2$  mass-squared matrix spanning  $\sqrt{2}\text{Re}(\phi_0, \phi_3)$  is

$$M_R^2 = \begin{pmatrix} 2(\lambda_1 + \lambda_2)c^2 + (1/2)\lambda_4(3sc + s^3/c) & 2(\lambda_1 - \lambda_2 + \lambda_3)sc + (3/2)\lambda_4(c^2 - s^2) \\ 2(\lambda_1 - \lambda_2 + \lambda_3)sc + (3/2)\lambda_4(c^2 - s^2) & 2(\lambda_1 + \lambda_2)s^2 - (1/2)\lambda_4(3sc + c^3/s) \end{pmatrix} v_D^2. \quad (14)$$

Let  $\zeta = \sqrt{2}\text{Re}(c\phi_0 + s\phi_3)$  and  $\phi_R = \sqrt{2}\text{Re}(s\phi_0 - c\phi_3)$ , then they are mass eigenstates, using the identity of Eq. (9), with masses

$$M_\zeta^2 = [2\lambda_1 + \lambda_3 + \frac{\cos^2 2\theta}{\cos 4\theta}(2\lambda_2 - \lambda_3)]v_D^2, \quad (15)$$

$$M_{\phi_R}^2 = \frac{-1}{\cos 4\theta}(2\lambda_2 - \lambda_3)v_D^2. \quad (16)$$

Hence  $\langle \zeta \rangle = \sqrt{2}v$  and  $\langle \phi_R \rangle = 0$ , with the latter (but not the former) connected to  $\phi_I$  through  $X_3$ . This has the important consequence of the emergence of an extra  $Z_2$  symmetry, under which  $\phi_{R,I}$  are odd and  $\zeta, \eta$  are even. As for the dark gauge bosons,  $X_1 \pm iX_2$  are odd and  $X_3$  is even.

The physical scalars are now contained in  $\phi_{0,1,2,3}$  as follows.

$$\phi_0 \rightarrow cv_D + \frac{1}{\sqrt{2}}(c\zeta + s\phi_R) + \frac{is}{\sqrt{2}}\phi_I, \quad (17)$$

$$\phi_1 \rightarrow s\eta, \quad \phi_2 \rightarrow c\eta^*, \quad (18)$$

$$\phi_3 \rightarrow sv_D + \frac{1}{\sqrt{2}}(s\zeta - c\phi_R) + \frac{ic}{\sqrt{2}}\phi_I. \quad (19)$$

The gauge-scalar interactions are

$$\begin{aligned} \mathcal{L}_{int}^{gs} = & \frac{3}{4}g_D X_3(\phi_R \partial \phi_I - \phi_I \partial \phi_R) + \frac{i}{2}g_D X_3(\eta \partial \eta^* - \eta^* \partial \eta) \\ & + \frac{\sqrt{3}}{2}ig_D \left[ \frac{X_1 + iX_2}{\sqrt{2}}(\phi_R - i\phi_I) \partial \eta - \frac{X_1 - iX_2}{\sqrt{2}}(\phi_R + i\phi_I) \partial \eta^* \right] \\ & - \frac{\sqrt{3}}{2}ig_D \left[ \frac{X_1 + iX_2}{\sqrt{2}}\eta \partial(\phi_R - i\phi_I) - \frac{X_1 - iX_2}{\sqrt{2}}\eta^* \partial(\phi_R + i\phi_I) \right] \\ & + \frac{3}{8}g_D^2(3X_3^2 + X_1^2 + X_2^2)(2\sqrt{2}v_D\zeta + \zeta^2 + \phi_R^2 + \phi_I^2) + \frac{1}{4}g_D^2(X_3^2 + 7X_1^2 + 7X_2^2)|\eta|^2 \\ & - \sqrt{3}g_D^2 X_3 \left( \frac{X_1 + iX_2}{\sqrt{2}} \right) (\phi_R - i\phi_I)\eta - \sqrt{3}g_D^2 X_3 \left( \frac{X_1 - iX_2}{\sqrt{2}} \right) (\phi_R + i\phi_I)\eta^* \\ & + \sqrt{\frac{3}{2}}g_D^2(\sqrt{2}v_D + \zeta) \left[ \left( \frac{X_1 - iX_2}{\sqrt{2}} \right)^2 \eta + \left( \frac{X_1 + iX_2}{\sqrt{2}} \right)^2 \eta^* \right]. \end{aligned} \quad (20)$$

Let  $x = \sin^2 2\theta$ , then

$$M_{\phi_R}^2 = \frac{1}{2x-1}(2\lambda_2 - \lambda_3)v_D^2, \quad (21)$$

$$M_{\phi_I}^2 = -(2\lambda_2 + \lambda_3)v_D^2 + M_{\phi_R}^2, \quad (22)$$

$$M_\eta^2 = \frac{2}{3}\lambda_2 v_D^2 + \frac{1}{2}M_{\phi_I}^2, \quad (23)$$

$$M_\zeta^2 = 2\lambda_1 v_D^2 - \frac{1}{2}M_{\phi_I}^2 = 2\lambda_D v_D^2. \quad (24)$$

Inverting the above,

$$\lambda_1 v_D^2 = \frac{1}{2}M_\zeta^2 + \frac{1}{4}M_{\phi_I}^2, \quad (25)$$

$$\lambda_2 v_D^2 = \frac{3}{2}M_\eta^2 - \frac{3}{4}M_{\phi_I}^2, \quad (26)$$

$$\lambda_3 v_D^2 = M_{\phi_R}^2 + \frac{1}{2}M_{\phi_I}^2 - 3M_\eta^2, \quad (27)$$

$$xM_{\phi_R}^2 = 3M_\eta^2 - M_{\phi_I}^2. \quad (28)$$

## B. Dark Sector Interactions with the Standard Model

With the addition of the Standard Model (SM) Higgs doublet  $H$  which is a singlet under the dark gauge  $SU(2)$ , the complete scalar interactions are then given by

$$\begin{aligned} -\mathcal{L}_{int} = & \frac{M_\zeta^2}{2v_D^2} \left[ \frac{v_D \zeta^3}{\sqrt{2}} + \frac{1}{8}\zeta^4 + \frac{1}{8}(\phi_R^2 + \phi_I^2)(\phi_R^2 + \phi_I^2 + 4|\eta|^2) \right] + \left( \frac{M_\zeta^2}{2v_D^2} + \frac{M_{\phi_R}^2}{v_D^2} \right) \left[ \frac{v_D \zeta}{\sqrt{2}} + \frac{1}{4}\zeta^2 \right] \phi_R^2 \\ & + \left( \frac{M_\zeta^2}{2v_D^2} + \frac{M_\eta^2}{v_D^2} \right) \left[ \frac{v_D \zeta}{\sqrt{2}} + \frac{1}{4}\zeta^2 \right] |\eta|^2 + \left( \frac{M_\zeta^2}{2v_D^2} + \frac{3M_\eta^2}{v_D^2} - \frac{M_{\phi_R}^2}{v_D^2} \right) \left[ \frac{v_D \zeta}{\sqrt{2}} + \frac{1}{4}\zeta^2 \right] \phi_I^2 \\ & + \left( \frac{M_\zeta^2}{4v_D^2} + \frac{M_\eta^2}{3v_D^2} \right) |\eta|^4 + \frac{1}{3\sqrt{3}} \left( \frac{2M_{\phi_R}^2}{v_D^2} - \frac{3M_\eta^2}{v_D^2} \right) \left[ v_D + \frac{\zeta}{\sqrt{2}} \right] (\eta^3 + \eta^{*3}) \\ & + \lambda_{H\phi} (H^\dagger H) (\Phi^\dagger \Phi) - \mu_H^2 (H^\dagger H) + \frac{\lambda_H}{2} (H^\dagger H)^2, \end{aligned} \quad (29)$$

where

$$(H^\dagger H) = \left( v_H + \frac{h}{\sqrt{2}} \right)^2, \quad (30)$$

$$(\Phi^\dagger \Phi) = \left( v_D + \frac{\zeta}{\sqrt{2}} \right)^2 + \frac{1}{2}\phi_R^2 + \frac{1}{2}\phi_I^2 + |\eta|^2. \quad (31)$$

From the above, it is clear that the scalar portal coupling  $\lambda_{H\phi}$  is the only connection between the dark and SM sectors. It allows  $h$  to couple to  $|\eta|^2$ ,  $\phi_{R,I}^2$ , as well as  $\zeta^2$ , and leads to the mixing between  $h$  and  $\zeta$ , with mass-squared matrix given by

$$\mathcal{M}_{h\zeta}^2 = \begin{pmatrix} 2\lambda_H v_H^2 & 2\lambda_{H\phi} v_H v_D \\ 2\lambda_{H\phi} v_H v_D & 2\lambda_D v_D^2 \end{pmatrix}. \quad (32)$$

This mixing also implies that the dark gauge bosons  $X_{1,2,3}$  are also coupled to the SM through  $\lambda_{H\phi}$ .

The  $\lambda_{H\phi}$  coupling allows the  $Z_3 \times Z_2$  dark matter to scatter off nucleons through the SM Higgs boson. It is required to be very small, of order  $10^{-4}$ , to agree with present experimental data. However, it should also be big enough so that the physical scalar which is mostly  $\zeta$  could decay rapidly through its small  $h$  component to SM particles. For the purpose of discussing the relic abundance,  $\lambda_{H\phi}$  may be neglected, as in our previous study [5]. Under the residual dark  $Z_3 \times Z_2$  symmetry, the SM particles as well as  $\zeta$  and  $X_3$  do not transform, whereas

$$\eta \sim (\omega, +), \quad \phi_{R,I} \sim (1, -), \quad (X_1 - iX_2)/\sqrt{2} \sim (\omega, -). \quad (33)$$

This means that there are at least two stable dark-matter components. We will assume that  $\eta$  is the lightest, and  $\phi_I$  the second lightest, with both annihilating to  $\zeta$ . We choose our input parameters to be

$$g_D, v_D, x, \lambda_{H\phi}, M_\zeta, M_\eta, M_{\phi_I},$$

with the mass hierarchy

$$M_{\phi_R} > M_{X_3} > M_{X_{1,2}} > M_{\phi_I} > M_\eta > M_\zeta. \quad (34)$$

We discuss the details of the resulting DM phenomenology in the upcoming section.

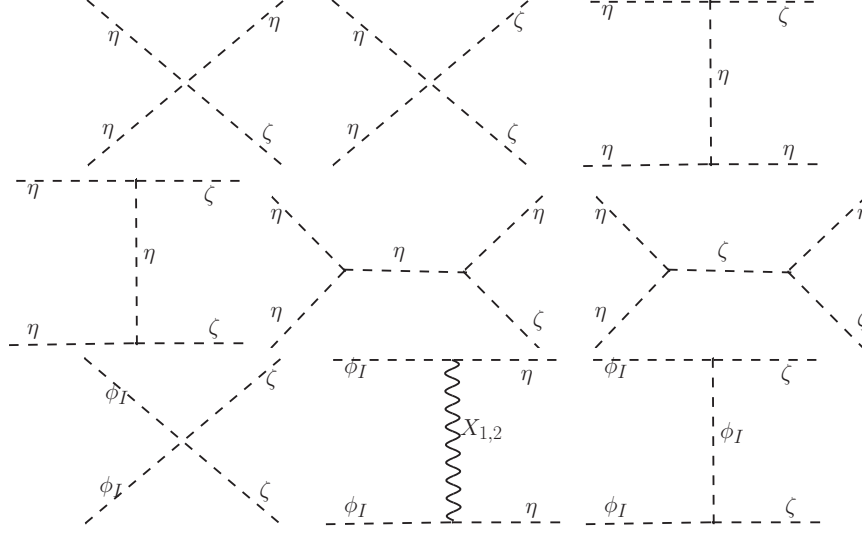


FIG. 1: Dominant Semi-annihilation and annihilation channels for DM components  $\eta$  and  $\phi_I$ .

### III. DARK MATTER PHENOMENOLOGY

As mentioned above, we have a natural two-component DM model due to the residual  $Z_3 \times Z_2$  discrete symmetry from the spontaneous breaking of dark gauge  $SU(2)$  by a Higgs quadruplet. To discuss the relic density of two-component dark matter [13–17] quantitatively, we first write the coupled Boltzmann equations (BEs) for comoving number densities of the two DM candidates which we assume to be  $\eta$  and  $\phi_I$  respectively. We have assumed that  $\eta$  is the lightest  $Z_3$  odd particle in the spectrum and is absolutely stable. On the other hand, due to the unbroken  $Z_2$  symmetry,  $\phi_I$  is also stable along with  $\eta$ . In Fig. 1, we show the dominant Feynman diagrams contributing to the annihilation and semi-annihilation processes of both  $\eta$  and  $\phi_I$ . Since  $\phi_I$  is neutral under  $Z_3$  it gives rise to typical annihilation channels into lighter particles while  $\eta$ , being charged under  $Z_3$ , also has semi-annihilation processes like  $\eta\eta \rightarrow \eta\zeta$ , typical of  $Z_3$  dark matter. We have assumed that  $X_{1,2,3}$ ,  $\phi_R$  are heavier and hence these final states will not contribute to the relic density calculation. Also, as mentioned earlier, the Higgs portal coupling  $\lambda_{H\phi}$  is assumed to be small so that the annihilation processes to SM final



states remain sub-dominant. However, this coupling cannot be arbitrarily small as the dark sector gets thermalised with the SM by virtue of Higgs portal interactions only. This leads to a lower bound on  $\lambda_{H\phi}$  from the requirement of dark sector thermalisation. Considering the point-like interaction  $\zeta\zeta \rightarrow hh$  with a cross-section  $\sigma \approx \lambda_{H\phi}^2/(32\pi s)$ , one can find the lower bound on  $\lambda_{H\phi}$  by demanding the rate of interaction to be greater than the Hubble expansion rate at some high temperature  $T$ . This leads to  $n^{\text{eq}}\langle\sigma v\rangle(T) > \mathbf{H}(T) = 1.66\sqrt{g_*}T^2/M_{\text{Pl}}$ . Demanding the dark sector to thermalise with the SM above the TeV scale ( $T \geq 1\text{ TeV}$ ) leads to  $\lambda_{H\phi} \gtrsim 10^{-7}$ . Choosing it to be very small, however, can lead to very early DM-SM decoupling. This requires the tracking of dark sector temperature evolution till the epoch of dark sector freeze-out. In this work, we consider  $\lambda_{H\phi}$  to be in the ballpark of  $10^{-4} - 10^{-3}$  and assume the dark sector and the SM baths to evolve with a common temperature.

Choosing the variable to be  $x_i = (M_i/T)$  with  $i = 1, 2$  for  $\eta, \phi_I$  respectively, the BEs in the limit of two stable dark matter candidates with the possible annihilations specified above, can be written as

$$\begin{aligned} \frac{dY_\eta}{dx_1} = \frac{\beta s}{\mathbf{H}x_1} & \left( -\langle\sigma(\eta\eta \rightarrow \text{SM SM})v_{\text{rel}}\rangle \left[ Y_\eta^2 - (Y_\eta^{\text{eq}})^2 \right] - \langle\sigma(\eta\eta \rightarrow \zeta\zeta)v_{\text{rel}}\rangle \left[ Y_\eta^2 - (Y_\eta^{\text{eq}})^2 \right] \right. \\ & - \langle\sigma(\eta\eta \rightarrow \eta h)v_{\text{rel}}\rangle \left[ Y_\eta^2 - Y_\eta^{\text{eq}}Y_\eta \right] - \langle\sigma(\eta\eta \rightarrow \eta\zeta)v_{\text{rel}}\rangle \left[ Y_\eta^2 - Y_\eta^{\text{eq}}Y_\eta \right] \\ & \left. + \langle\sigma(\phi_I\phi_I \rightarrow \eta\eta)v_{\text{rel}}\rangle \left[ Y_{\phi_I}^2 - \frac{(Y_{\phi_I}^{\text{eq}})^2}{(Y_\eta^{\text{eq}})^2} Y_\eta^2 \right] \right), \end{aligned} \quad (35)$$

$$\begin{aligned} \frac{dY_{\phi_I}}{dx_2} = \frac{\beta s}{\mathbf{H}x_2} & \left( -\langle\sigma(\phi_I\phi_I \rightarrow \text{SM SM})v_{\text{rel}}\rangle \left[ Y_{\phi_I}^2 - (Y_{\phi_I}^{\text{eq}})^2 \right] - \langle\sigma(\phi_I\phi_I \rightarrow \zeta\zeta)v_{\text{rel}}\rangle \left[ Y_{\phi_I}^2 - (Y_{\phi_I}^{\text{eq}})^2 \right] \right. \\ & \left. - \langle\sigma(\phi_I\phi_I \rightarrow \eta\eta)v_{\text{rel}}\rangle \left[ Y_{\phi_I}^2 - \frac{(Y_{\phi_I}^{\text{eq}})^2}{(Y_\eta^{\text{eq}})^2} Y_\eta^2 \right] \right), \end{aligned} \quad (36)$$

where  $Y_x = (n_x/s)$  denotes comoving number density for  $x \equiv \eta, \phi_I$  with

$$\beta(T) = 1 + \frac{1}{3} \frac{T}{g_s(T)} \frac{dg_s(T)}{dT}$$

and  $\mathbf{H}$  being the Hubble parameter. The first term of the right hand side of Eq. (35) shows the annihilation to the SM final states whereas the second, third and fourth terms show the

annihilation to  $\zeta\zeta$ , semi-annihilation to Higgs and  $\zeta$  respectively. The last term represents the conversion processes between the two dark matter particles. Similarly, the first term of the right hand side of Eq. (36) is for the annihilation to the SM final states and the second and the third terms are for the annihilation to  $\zeta$  and conversion to  $\eta$  respectively. Among all these processes the two  $\zeta$  final state and the semi-annihilation processes give the dominant contribution to the relic density due to the chosen mass hierarchy as well as small Higgs portal interactions. In order to calculate the thermally averaged annihilation cross-sections and solve the above BEs numerically, we use `micrOMEGAs` [18].

Let us discuss the numerical results of the model. As discussed above, we have two different components of stable dark matter in this scenario, the lightest  $Z_3$ -charged particle  $\eta$  and the lightest  $Z_2$ -odd particle  $\phi_I$ . However, in this study we have restricted ourselves to the regime where  $M_\eta$  is smaller than  $M_{\phi_I}$ . For our analysis, we have considered the mixing between the dark sector and the SM to be small governed by the smallness of  $\lambda_{H\phi}$ . We consider the two DM masses to be free parameters with  $M_\eta < M_{\phi_I}$ . We also choose the remaining free parameters  $g_D, v_D, x, \lambda_{H\phi}, M_\zeta$  in a way which maintains the dark sector mass hierarchy in Eq. (34). In Fig. 2, we have shown the total DM relic density as function of  $M_\eta$  for three different benchmark values of  $M_\zeta$ . One can note that total relic density decreases with decreasing mass splitting between  $M_\eta$  and  $M_\zeta$ . For a fixed value of  $M_\eta$ , as we increase  $M_\zeta$  in order to decrease the mass splitting  $M_\eta - M_\zeta$ , it increases the scalar interactions of  $\eta$  as seen from Eq. (29) enhancing its annihilation rate thereby decreasing the relic abundance. It is noteworthy that, for the chosen mass hierarchy of  $X_{1,2}, \phi_R, \eta$ , the total DM relic is dominated by  $\eta$  as strong annihilation and conversion rates of heavier DM candidate  $\phi_I$  reduces its relative abundance. In order to make it clear, we scan the parameter space for the chosen hierarchy. In Fig. 3, we have shown the allowed parameter space in  $M_\eta - M_\zeta$  plane from the observed total relic density constraints of dark matter. Color bar in

the left panel shows the variation of dark gauge boson ( $X_{1,2}$ ) mass whereas the same in the right panel shows the variation of relative relic abundance of  $\eta$  ( $R_\eta = \Omega_\eta/(\Omega_\eta + \Omega_{\phi_I})$ ). As seen from the right panel plot, the total relic density is dominated by  $\eta$  for the chosen mass hierarchy. This is due to large annihilation rate of  $\phi_I$  by virtue of its large coupling with  $\zeta$  for the chosen mass spectrum of different scalars, as seen from the scalar interactions in Eq. (29). We have also shown the region where  $M_\zeta$  is larger than  $M_\eta$  by the light shaded region. Since  $\zeta$  is the only new particle to which  $\eta$  can annihilate into apart from its annihilation into SM particles suppressed by small Higgs portal couplings, most of the relic satisfying points prefer  $M_\eta > M_\zeta$  to keep the annihilation rate into  $\zeta$  efficient.

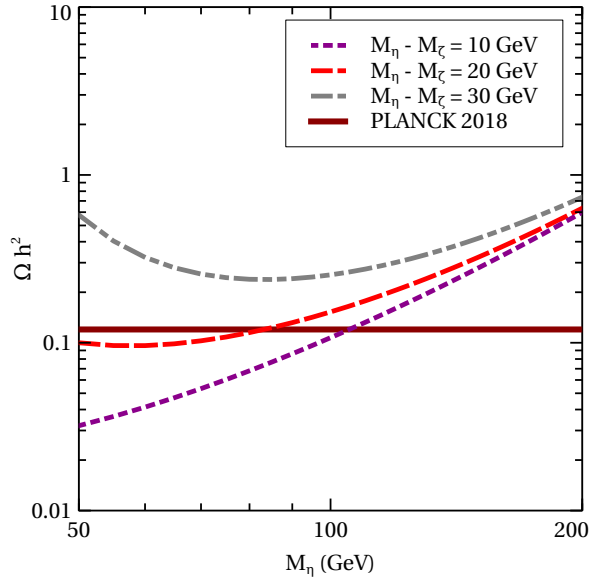


FIG. 2: Total relic density of dark matter as a function of  $M_\eta$  for three different mass splitting between  $M_\eta$  and  $M_\zeta$ .

We have chosen Higgs portal coupling  $\lambda_{H\phi} = 10^{-4}$  in the above analysis, which is sufficient to bring dark sector in thermal equilibrium with the SM while keeping the direct detection cross-section suppressed. For higher values of Higgs portal coupling, this model can also be tested in the ongoing and future direct detection experiments [19, 20]. Due to Higgs portal interactions, dominant DM component namely,  $\eta$  can scatter off nucleon at tree level leading

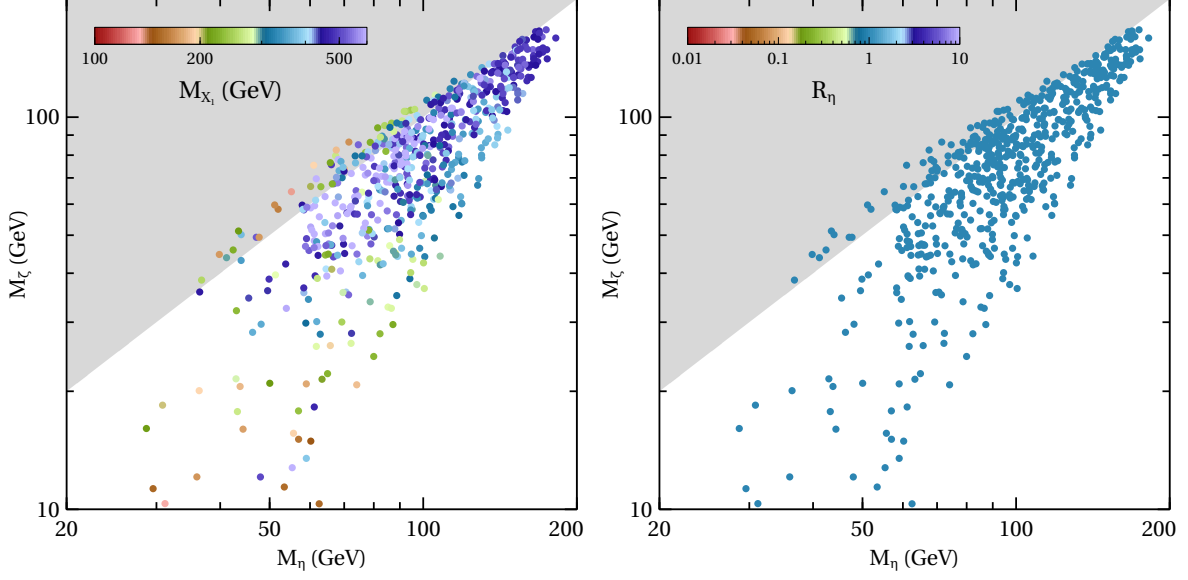


FIG. 3: Allowed parameter space in  $M_\eta - M_\chi$  plane from total DM relic abundance criteria. Color bar in the left (right) panel shows the variation of dark gauge boson mass  $M_{X_1}$  (relative relic abundance of  $\eta$  given by  $R_\eta = \Omega_\eta/(\Omega_\eta + \Omega_{\phi_I})$ ).

to spin-independent DM-nucleon scattering cross-section tightly constrained by experiments. In Fig. 4, we show the spin-independent DM-nucleon cross-section as a function of  $M_\eta$ . The current constraint from LZ [19] and future sensitivity of DARWIN [20] are shown as shaded regions. The points corresponding to  $\lambda_{H\phi} = 10^{-4}$  correspond to the data points shown in Fig. 3. Clearly, they remain even out of reach at future experiments. We check that a larger Higgs portal coupling  $\lambda_{H\phi} = 10^{-3}$  which is still small enough not to alter the relic density analysis discussed above, can bring the direct detection rate within current and future experimental reach for certain range of DM masses, keeping the model verifiable.

#### IV. CONCLUSION

We have studied a gauge  $SU(2)$  symmetry as the origin of dark matter where a scalar quadruplet plays the role of breaking the gauge symmetry spontaneously into a residual  $Z_3 \times$

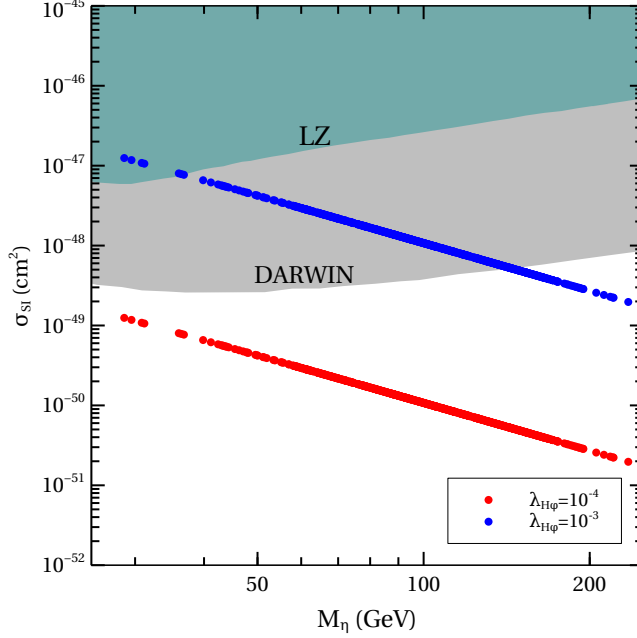


FIG. 4: Spin-independent direct detection cross-section as a function of DM mass for two different values of Higgs portal coupling  $\lambda_{H\phi}$ .

$Z_2$  symmetry responsible for stabilising dark matter. This framework not only gives rise to a fundamental origin of  $Z_3$  dark matter, but also offers a rich phenomenology due to existence of a second DM candidate, stabilised by a  $Z_2$  symmetry. We have studied the thermal DM scenario considering dark sector to reach thermal equilibrium with the standard model by virtue of Higgs portal couplings. Dark matter relic abundance is primarily governed by interactions within the dark sector like annihilation, semi-annihilation and conversions with the annihilation into SM particles being sub-dominant due to small Higgs portal couplings required to obey direct detection constraints. Suitable choices of Higgs portal couplings can lead to observable direct detection cross-section keeping the model verifiable. While we have assumed specific mass hierarchy among dark sector particles to study the phenomenology of two scalar DM candidates, other possible mass hierarchies can lead to mixed type of DM consisting of both dark scalar and dark gauge bosons. We leave such detailed studies to future works.

## Acknowledgments

This work was supported in part by the U. S. Department of Energy Grant No. DE-SC0008541. The work of DN is partly supported by National Research Foundation of Korea (NRF)'s grants with grants No. NRF-2019R1A2C3005009(DN).

---

- [1] B.-L. Young, Front. Phys. (Beijing) **12**, 121201 (2017), [Erratum: Front.Phys.(Beijing) 12, 121202 (2017)].
- [2] E. Ma, Phys. Rev. Lett. **115**, 011801 (2015), 1502.02200.
- [3] E. Ma, Phys. Lett. B **809**, 135736 (2020), 1912.11950.
- [4] T. Hambye, JHEP **01**, 028 (2009), 0811.0172.
- [5] D. Borah, E. Ma, and D. Nanda, Phys. Lett. B **835**, 137539 (2022), 2204.13205.
- [6] E. Ma, LHEP **02**, 01 (2018), 1804.00374.
- [7] G. Etesi, J. Math. Phys. **37**, 1596 (1996), hep-th/9706029.
- [8] A. Adulpravitchai, A. Blum, and M. Lindner, JHEP **09**, 018 (2009), 0907.2332.
- [9] K. Agashe and G. Servant, Phys. Rev. Lett. **93**, 231805 (2004), hep-ph/0403143.
- [10] E. Ma, Phys. Lett. B **662**, 49 (2008), 0708.3371.
- [11] B. Batell, Phys. Rev. D **83**, 035006 (2011), 1007.0045.
- [12] S. F. King and Y.-L. Zhou, JHEP **11**, 173 (2018), 1809.10292.
- [13] Q.-H. Cao, E. Ma, J. Wudka, and C. P. Yuan (2007), 0711.3881.
- [14] K. M. Zurek, Phys. Rev. **D79**, 115002 (2009), 0811.4429.
- [15] Z.-P. Liu, Y.-L. Wu, and Y.-F. Zhou, Eur. Phys. J. C **71**, 1749 (2011), 1101.4148.
- [16] G. Belanger and J.-C. Park, JCAP **1203**, 038 (2012), 1112.4491.
- [17] A. Adulpravitchai, B. Batell, and J. Pradler, Phys. Lett. B **700**, 207 (2011), 1103.3053.
- [18] G. Bélanger, F. Boudjema, A. Pukhov, and A. Semenov, Comput. Phys. Commun. **192**, 322 (2015), 1407.6129.
- [19] J. Aalbers et al. (LUX-ZEPLIN) (2022), 2207.03764.
- [20] J. Aalbers et al. (DARWIN), JCAP **11**, 017 (2016), 1606.07001.